Article
Vol. 26, No. 6, p. 731–747, December 2022
https://doi.org/10.1007/s12303-022-0020-3
pISSN 1226-4806 eISSN 1598-7477
Geosciences Journal GJ

Improvement of fluid penetration in soil by plasma blasting

Hyun-Sic Jang[1], In-Joon Baek[1], Jae-Yong Song[2], Geun-Chun Lee[2], and Bo-An Jang[1]*

[1]Department of Geophysics, Kangwon National University, 1, Kangwondaehak-gil, Chuncheon-si, Gangwon-do 24341, Republic of Korea
[2]SanHa Engineering & Construction Co. Ltd., 124, Sagimakgol-ro, Jungwon-gu, Seongnam-si, Gyeonggi-do 13207, Republic of Korea

ABSTRACT: Plasma blasting by high-voltage arc discharge was performed in laboratory-scale soil samples to investigate fluid penetration. A plasma blasting device with a large-capacity capacitor and columnar soil samples with a diameter of 80 cm and a height of 60 cm were prepared. The columnar soil samples were made of sand and silt mixed in a 7:3 ratio (the A samples) or a 9:1 ratio (the B samples). When fluid was injected by pressure without plasma blasting, fluid penetrated into the soil only near the borehole, and the penetration area ratio was less than 10%. In further tests, fluid was injected by plasma blasting with different discharge energies of 1–27 kJ. When plasma blasting was performed once in the A samples, the penetration area ratios of the fluid were 16–25%; after five consecutive blasts, the penetration area ratios were 30–48%. When five consecutive plasma blasts were carried out on the B samples, the fluid penetration area ratios were 33–72%. This difference indicates that the fluid penetration area increases with higher discharge energy of plasma blasting and with a greater number of blasts. The fluid penetration radius was calculated to assess the fluid penetration volume. When the fluid was injected by hydraulic pressure only, the penetration radius was 9–12.4 cm, whereas the penetration radius was 27–33.2 cm when blasting was performed five times. The radius was increased by up to 200% by plasma blasting. In the field tests, the fluid injection in the test hole subjected to plasma blasting was greater by about 170% compared with the control test hole, in which the fluid was injected only by hydraulic pressure. In addition, the electrical resistivity around the test hole subjected to plasma blasting was markedly lower, and fluid diffused from this test hole to a minimum radius of 2 m. These results indicate that a cleaning agent will penetrate further and the remediation efficiency of contaminated soil will be improved if plasma blasting is applied for in situ cleaning of low-permeability contaminated soil.

Key words: plasma blasting, discharge energy, fluid penetration, contaminated soil, remediation of soil contamination

Manuscript received June 6, 2022; Manuscript accepted August 10, 2022

1. INTRODUCTION

Oil contamination of soil results in soil and water pollution through groundwater and air pollution by volatile pollutants. To restore such soil to its original state, considerable time and money must be invested, so an effective technology for treating contaminated soil is required. Contaminated soil treatment technologies are divided into on-site treatment and off-site treatment depending on whether the soil can be treated within the contaminated site. On-site treatment is divided into in situ remediation, which purifies contaminated soil directly in the ground, and ex situ remediation, which excavates and treats contaminated soil (EPA, 2004, 2007).

In situ remediation is preferred because it is relatively cheaper than ex situ remediation. Physical and chemical treatment techniques are commonly used in preference to thermal treatment, which consumes large amounts of energy and has the potential to cause secondary air pollution (Yang and Lee, 2007; Fawzy, 2008). Of in situ remediation methods, soil cleaning is a physicochemical purification method in which a cleaning solution injected through a well both desorbs pollutants in the soil and separates pollutants through mechanical friction under high pressure. This method has a fast purification time and can be used for purification of highly contaminated soil by selecting various additives depending on the pollutants. This method does not require excavation of the soil and has the advantage of being able to purify the soil and groundwater together without

*Corresponding author:
Bo-An Jang
Department of Geophysics, Kangwon National University, 1, Kangwondaehak-gil, Chuncheon-si, Gangwon-do 24341, Republic of Korea
Tel: +82-10-3281-6137, E-mail: bajang@kangwon.ac.kr

disturbing the environment. However, when the soil washing method is used for soil with low permeability, such as granite weathered soil, the permeation rate of the fluid is low and the purification treatment efficiency is poor; thus, this treatment is used as an auxiliary method rather than the main method. Therefore, to apply soil cleaning as the main method, improving the permeability of the soil is essential, because cleaning solutions such as surfactants do not move, but instead remain in the soil and cause secondary contamination if the soil permeability is low (Huguenot et al., 2015; Kang et al., 2017; Liu et al., 2021). Hydraulic fracturing and pneumatic fracturing are commonly applied to increase the permeability of soil. These methods apply a static load to the inside of the soil by means of high-pressure water and air. The resulting cracks improve the permeability of the soil (EPA, 1995; Frank and Barkley, 1995; Schuring et al., 1996; Venkatraman et al., 1998; Suthersan, 1999; Lhotský et al., 2021). However, this static load is rapidly dissipated along surfaces of minimum resistance, such as crack surfaces, resulting in a type of fluid channeling that forms a large-scale crack in a specific direction (Christiansen and Wood, 2006). Because the purifying agent penetrates into the soil only through the fluid channel, some contaminants remain, and additional purification is inevitably required. Therefore, an effective method that can three-dimensionally diffuse the purification agent throughout the contaminated soil is required.

Recently, remediation using an electrical current has been extensively studied. The electrokinetic remediation method applies a DC voltage to wet contaminated soil to promote electromigration, electro-osmosis, and electrophoresis to enhance the flow of the cleaning agent and evaporation of pollutants (Li et al., 1996; Rosestolato et al., 2015; Santos et al., 2016; Ferrucci et al., 2017). Dielectrical barrier discharge and corona discharge, which induce ultraviolet radiation, radical reaction, and thermal dissociation, clean contaminated soil by oxidization or reduction (Li et al., 2011; Zhan et al., 2018; Aggelopoulos et al., 2020). However, there are many practical difficulties when applying these methods to large-scale in situ remediation rather than at the laboratory scale, such as low efficiency versus time, secondary pollution caused by residual contaminants, chemical reaction inefficiency in high-moisture soil, and the necessity for large-scale electrode installation.

A new plasma blasting method using a high-voltage arc discharge has been introduced as a ground-breaking technology. Plasma blasting uses relatively low energy to effectively form cracks in the ground while minimizing noise, vibration, and rock scattering, thus providing a possible alternative to pneumatic fracturing and hydraulic fracturing (Hammon et al., 2001; Chen et al., 2012; Riu et al., 2019). Improving the permeability and fluid transfer efficiency of soil by using the shock waves generated by plasma blasting can be applied immediately at a large scale to contaminated soils and has the advantage of being linked to the existing in situ remediation method. As the shock wave caused by plasma blasting is not biased in a specific direction and generates a dynamic load evenly in the medium, when plasma blasting is applied to soil, the channeling that occurs during hydraulic fracturing or pneumatic fracturing does not take place; instead, a radial crack network is generated (Ikkurthi et al., 2002; Baltazar-Lopez et al., 2009; Maurel et al., 2010; Jang et al., 2020). The radial cracks generated during plasma blasting and fluid transfer based on strong pressure have the advantage of minimizing residual contaminants in the soil, so the remediation efficiency is expected to be maximized.

In this study, laboratory tests and field tests were conducted to verify the effect of fluid penetration by plasma blasting, and, ultimately, to assess the possibility of applying plasma blasting for in situ remediation. For the laboratory test, a white paint solution was used to easily check the range of fluid diffusion in the soil. The fluid penetration rates generated by fluid injection involving only hydraulic pressure and with plasma blasting were compared. By applying different discharge voltages and numbers of blasts to two types of soil samples with different permeability values, the effect of improving permeability for soil was reviewed, and the effects of voltage and number of discharges on permeability improvement were analyzed. The appropriate discharge voltage and number of discharges obtained based on the laboratory-scale test results were applied in field tests to measure the changes in the amount of fluid injected during plasma blasting. The range of fluid diffusion after plasma blasting was assessed through measurement of electrical resistivity.

2. THEORETICAL BACKGROUND OF PLASMA BLASTING

The states of matter can be divided into solid, liquid, and gas on the basis of the kinetic energy of the constituent molecules, which is controlled by the temperature. When a gas, which is the form of matter with the highest kinetic energy, is heated to a higher temperature, electrons escape from the nucleus and become free. At this time, the material has sufficiently high density to exhibit collective behavior, and because of the random thermal motion of ionized charged particles, it exhibits quasi-neutral characteristics, making the gas a fourth state of matter, i.e., a plasma. Plasma consists of charge carriers such as electrons, ions, and neutral gas molecules, so an electrical current can flow easily.

When a voltage over a certain limit is applied to an insulator, the dielectrical material acts as a conductor, causing dielectrical breakdown. As a result of insulation breakdown, the insulation

properties are lost and current flows: this process is called discharge. In the initial stage of the discharge, a local discharge occurs and a minute current flows. This phenomenon is collectively called partial discharge, local discharge, or incomplete discharge. If the voltage is further increased in this state, insulation breakdown occurs across the electrodes, and the electrode is completely connected to a discharge path with very high conductivity, resulting in electrical circuit breakdown or flashover (in which the current rapidly increases). Insulating materials can exist in solid, liquid, or gaseous form. When a high voltage is applied to a gas dielectrical, electrical circuit breakdown proceeds rapidly, and the gas particles collide with each other with very high energy, causing the atoms or molecules to lose electrons. This process is called ionization, and the vicinity of the electrode where the high-voltage discharge occurs becomes a plasma state, i.e., an ionized gas.

When a high voltage is applied between electrodes in water, the liquid insulation is broken and a strong electrical field is induced, and electrical energy is converted into thermal energy, causing electrolysis of water by Joule heating. For water to be electrolyzed to form microbubbles, a voltage exceeding a threshold energy must be applied. The threshold energy is generally several tens of Joules or more, and the generation of bubbles above the threshold energy depends on the magnitude of the applied voltage. When energy of several hundred Joules or more is applied, the bubbles continue to grow and fill the gaps between the electrodes, and the electrodes are placed between the gas dielectricals. At this time, the electrons are accelerated and the colliding water molecules are ionized and a local discharge occurs. If the voltage is further increased in this state, the electrons are further accelerated, and a large number of ions are generated by a chain reaction, resulting in arc discharge. Because of this electrical circuit breakdown, the gas in the bubble is in a plasma state. Because the high-temperature plasma reaching tens of thousands of degrees Celsius vaporizes the water around the electrode, a rapid volume expansion occurs. This expansion acts on the surrounding water, and because the water resists compression, a strong radial shock wave propagates to the surroundings.

3. PLASMA BLASTING DEVICE

A plasma blasting device accumulates high-voltage DC electricity in a large-capacity capacitor, and then generates

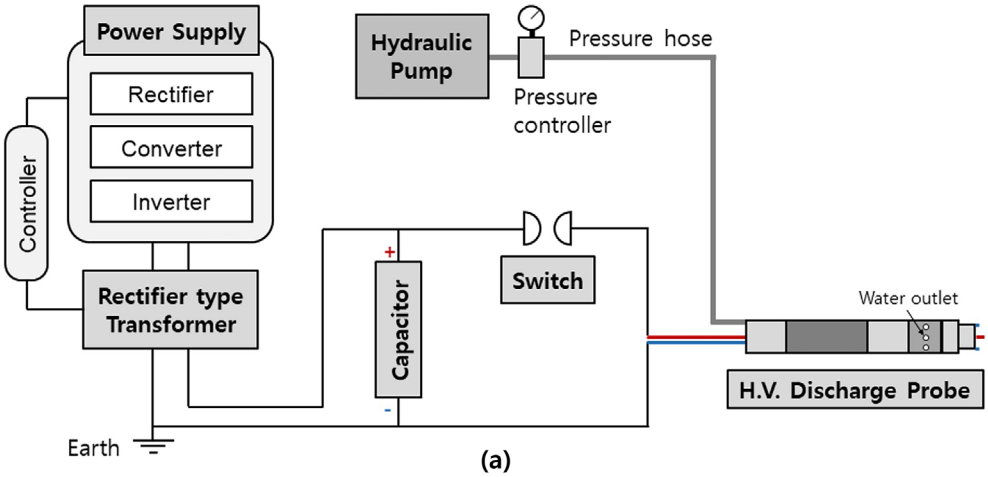

(b)

Fig. 1. (a) Schematic diagram and (b) photo of the plasma blasting device.

https://doi.org/10.1007/s12303-022-0020-3

explosive energy through an instantaneous high-energy pulse-arc discharge. This type of device has been used in several studies on plasma blasting (Touya et al., 2006; Best et al., 2008; Maurel et al., 2010; Chen et al., 2012; Zhu et al., 2013; Yan et al., 2016). The electrical energy (E) that can be accumulated in the capacitor is proportional to the square of the capacitor's capacitance (C) and the charging voltage (V), as given in Equation (1).

$$E = \frac{1}{2}CV^2. \quad (1)$$

The plasma blasting device used in this study consists of a power supply, a rectifier-type transformer, a capacitor, a spark-gap switch, a fluid pump, and a discharge probe (Fig. 1). The maximum charging voltage of the device is 50 kV and the maximum capacitance of the capacitor is 100 μF. Because the maximum charging voltage provided by the DC power supply and the transformer is 50 kV, the maximum electrical energy that can be stored is 125 kJ. The charging voltage can be set at values up to 50 kV using the control system, and the capacitance of the capacitor can be adjusted from 20 to 100 μF. Therefore, the capacitor can store electrical energy of 0.25–125 kJ.

The electrical energy stored in the capacitor is transferred to the discharge probe all at once by the operation of the spark-gap switch, and a high-voltage pulse-arc discharge occurs between the electrodes of the discharge probe. When such a discharge occurs in water, electrical energy is consumed in a small area around the electrode for a very short time. A high temperature is generated, plasma bubbles are formed, and powerful shock and pressure waves spread through the surrounding medium. A centrifugal pump with a maximum water pressure of 80 kPa was used to carry out fluid injection, and a flow meter and a pressure gauge were installed to measure the amount of injected fluid. The discharge probe is the distal end of the plasma blasting device and is where the actual blasting takes place. In the discharge part, there is an outlet through which fluid can be injected while the probe is fixed in the borehole, and a coaxial cylindrical electrode was used. A pneumatic packer is attached to the middle part of the probe.

4. PREPARATION OF COLUMNAR SOIL SAMPLES

Large columnar soil samples were prepared for laboratory testing. The column frame was 80 cm in diameter and 80 cm high. Considering the weight of heavy soil and to facilitate experimentation, the frame was made of a large iron plate, which was divided into two so that the column and soil could easily be separated after the test. Columnar soil samples were manufactured by repeating a constant compaction process in 5-cm-high units to produce a structure that was as homogeneous as possible, with a unit density of 1.8 g/cm^3 (Fig. 2). Each columnar soil sample consisted of an outer tube (the main body) and an inner tube, in which a plasma blasting probe was inserted. Soil was added to a height of 60 cm, and the inner tube was installed at a height of 20 cm from the floor. The soil used to fill the column was silty sand consisting of a mixture of sand and silt in a 7:3 ratio (sample A) and a 9:1 ratio (sample B). Seven samples of type A and three of type B were prepared. The permeability of sample A measured by variable head permeability testing was on average 1.21×10^{-4} cm/s. The permeability of sample B was on average 8.30×10^{-3} cm/s, approximately 70 times higher than

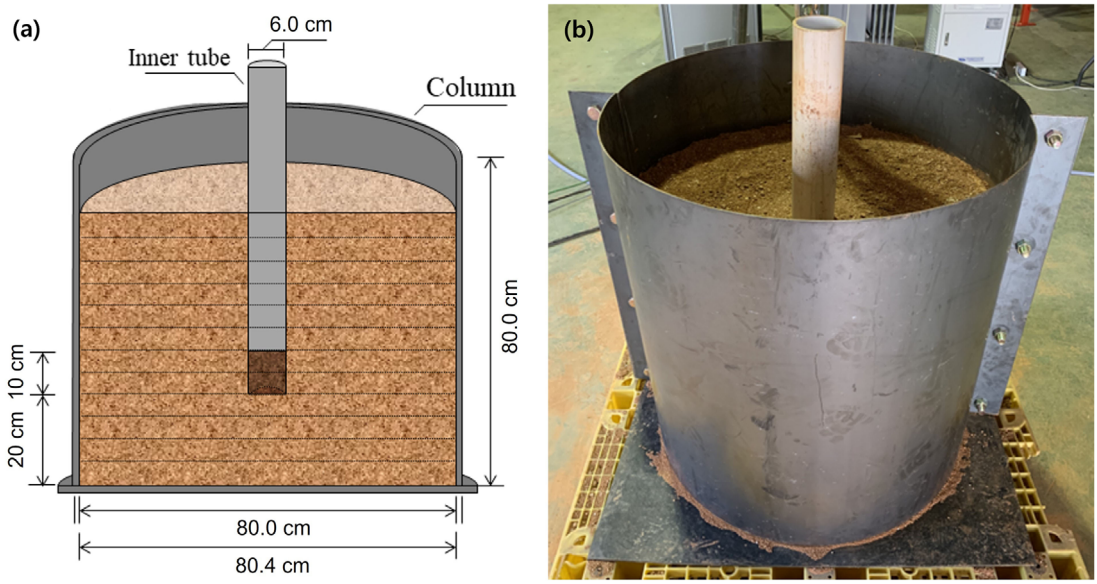

Fig. 2. (a) Schematic diagram and (b) photograph of a columnar soil sample.

Table 1. Properties of soil samples

	Natural water content (%)	Atterberg limits (%)		Specific gravity	Uniformity coefficient	Coefficient of curvature	Permeability (cm/s)	U.S.C.S
		LL	PI					
Sample A	14.2	NP	NP	2.658	143.9	1.2	1.21×10^{-4}	SM
Sample B	12.6	NP	NP	2.654	92.9	2.5	8.30×10^{-3}	SM

that of sample A. Thus, both samples were silty sand with poor permeability. The physical properties of samples A and B measured by laboratory tests are listed in Table 1.

5. GEOLOGY OF THE FIELD TEST AREA

The field test to measure the effect of plasma blasting on fluid penetration in the ground was conducted in a non-contaminated area in Chungju-si, Chungcheongbuk-do, Republic of Korea. The bedrock of this area is Jurassic biotite granite, with some Quaternary alluvial deposits (Park and Yeo, 1971; Fig. 3). The soil and rock sequence in borehole SH-1 was composed of alluvium from the surface to 3 m depth, then completely weathered soil at 3–4 m depth, highly weathered rock at 4–4.6 m depth, and moderately weathered rock at 4.6–10 m depth. The groundwater level lies at approximately 8.1 m depth. The alluvium consists of sand or loamy sand composed of 3.0–6.1% clay, 4.8–6.4% silt, and 87.5–92.2% sand. The bulk density is approximately 1.40–1.43 g/cm^3, and the water content is approximately 12.0–18.3%. The permeability of the alluvium is about 8.34×10^{-5} cm/sec.

For the field test, three boreholes (BH-1, BH-2, and BH-3) were drilled to a depth of 3 m in a triangular arrangement (Fig. 3). A stainless steel casing (inner diameter 65 mm) was installed from the surface to a depth of 2 m in the borehole, and a stainless slot screen was installed to a depth of 2–3 m.

6. LABORATORY-SCALE PLASMA BLASTING TEST

6.1. Discharge Characteristics During Plasma Blasting

Prior to the plasma blasting test, the voltage and current applied to the discharge probe during plasma blasting were measured to understand the high-voltage discharge characteristics of the plasma blasting device. The voltage was measured using a 6015A (Tektronix, USA) high-voltage probe, and a Model 2-0.01W/R current coil (Stangenes Industries Inc., USA) was used to measure the current. Both instruments were connected to a DPO 3032 digital oscilloscope (Tektronix) to acquire and record data in

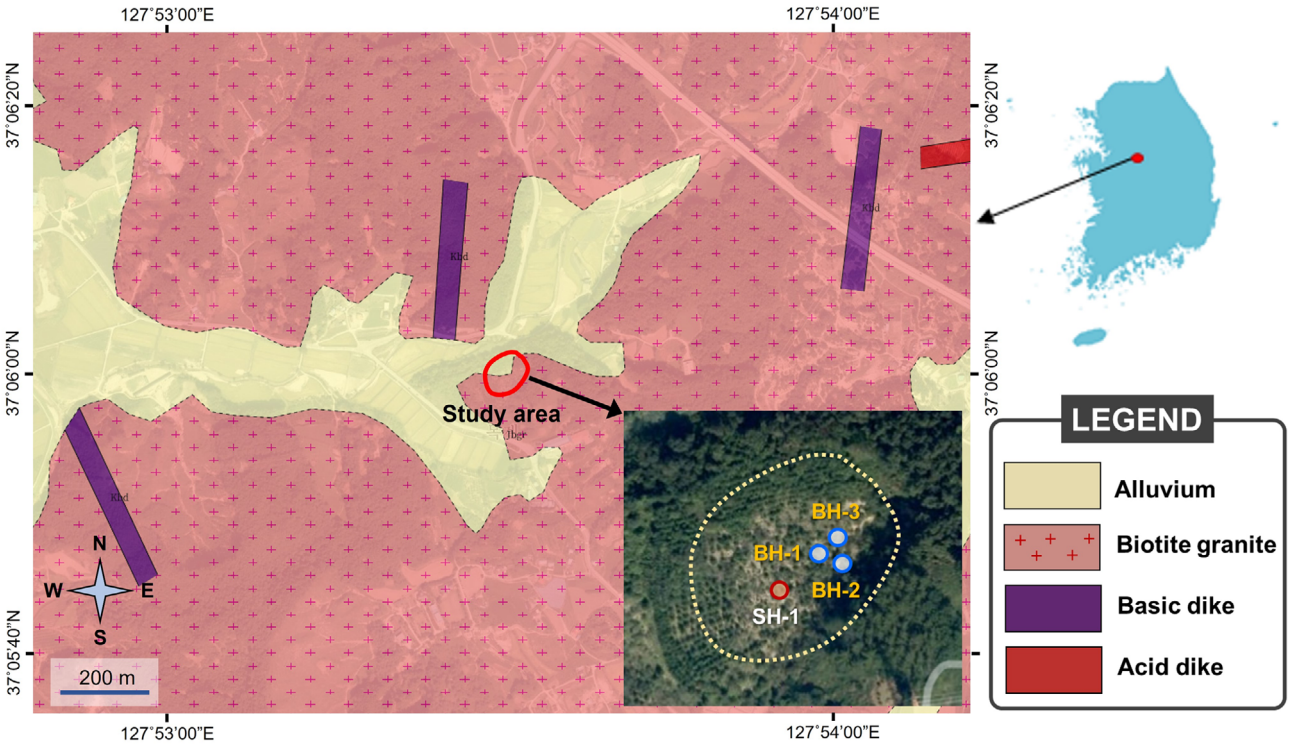

Fig. 3. Geological map of the study area and location of boreholes (scale 1:50,000).

https://doi.org/10.1007/s12303-022-0020-3

real time on a computer. The maximum capacitance of the plasma blasting device is 100 μF, but when all of the 100-μF capacity is used during plasma blasting, an excessively high current of 70 kA or more is generated, reducing the life of the storage battery and causing electrical damage to other devices. For this reason, the experiment was conducted with a capacitance of 60 μF.

The discharge characteristics were measured 25 times in increments of 5 kV from 10 to 35 kV. The voltage and current measured at the discharge probe and the discharge energy calculated from Equation (1) are illustrated in Figure 4. The voltage charged to the capacitor by the control system and the voltage measured in the probe during discharge were very similar, and exhibited a very good linear relationship ($R^2 = 0.996$; Fig. 4a). The discharge energy, when plotted against the charging voltage, increased parabolically, because the electrical energy is proportional to the square of the voltage (Fig. 4b). From the results, we confirmed that the plasma blasting apparatus can generate electrical energy of 40 kJ or more. The discharge voltage and the maximum current increased linearly as the charging voltage increased (Fig. 4c). These results show that the discharge characteristics can be sufficiently predicted and analyzed on the basis of only the charge voltage; thus, it is not necessary to continuously measure the discharge voltage during plasma blasting tests in future.

Representative voltage and current waveforms measured in the discharge probe are shown in Figure 5. The voltage waveform rose to the charged voltage level as dielectrical breakdown occurred in the spark gap, and then dropped sharply when a pulse-arc discharge took place at the discharge probe. The current waveform showed a very low value even after insulation breakdown took place in the spark gap until a discharge occurred at the probe electrode end, after which the current rapidly increased to its maximum value as soon as the discharge started. After the maximum current value, the discharge energy attenuated, during which the current did not disappear at once but gradually decreased. The discharge duration is the period from the start of the discharge until the current and voltage are finally attenuated: the higher the discharge voltage, the longer the discharge duration. In contrast, the discharge delay time, which is the time from the occurrence of electrical insulation breakdown in the spark gap

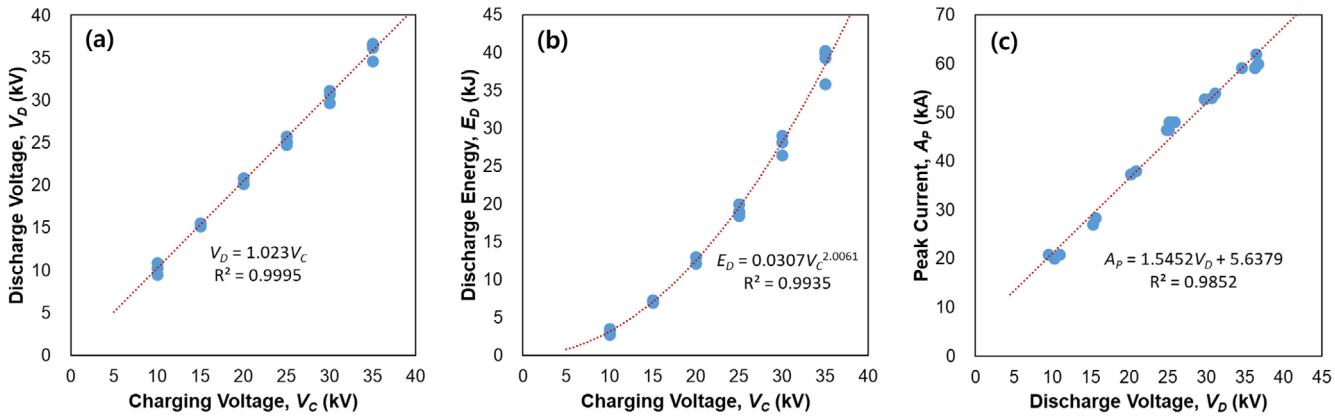

Fig. 4. Relations (a) between discharge voltage (V_D) and charging voltage (V_C), (b) between discharge energy (E_D) and charging voltage and (c) between peak current (A_P) and discharge voltage.

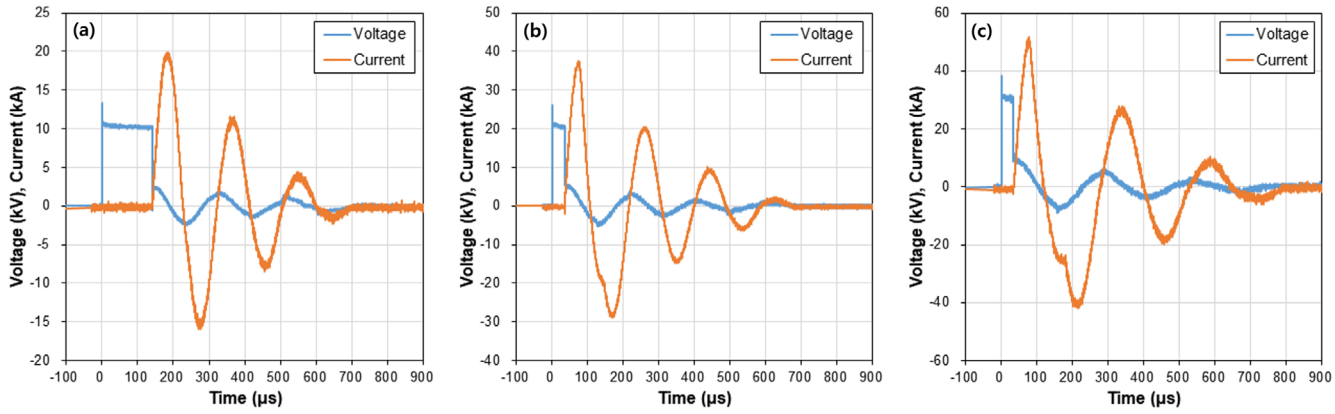

Fig. 5. Waveforms of voltage and current for discharge voltages of (a) 10 kV, (b) 20 kV and (c) 30 kV.

until the actual discharge in the discharge probe, becomes shorter as the voltage increases.

6.2. Laboratory-scale Fluid Injection Tests with Plasma Blasting

To check the effect of fluid penetration, plasma blasting was performed while injecting water containing white paint into columnar soil samples (samples A and B) with a pressure of approximately 50 kPa for 10 min. After the paint/water mixture injection experiment was completed, the soil samples were vertically incised to visually observe the penetration range in the soil samples. The fluid penetration area ratio was calculated by comparing the measured penetration cross-sectional area of the paint/water mixture with the total vertical cross-sectional area of the soil sample.

6.2.1. Fluid penetration with water pressure only

One sample A and one sample B were set as control samples and the paint/water mixture (hereafter referred to as the mixture) was injected for 10 min with only water pressure (i.e., without plasma blasting). The water pressure rose up to 50 kPa at the beginning of injection and a channel (water path) was formed inside the sample A (Fig. 6a). As the mixture flowed out of the upper part of the sample, the water pressure rapidly reduced to less than 10 kPa. After the test was completed, the sample was cut vertically and penetration of the mixture was observed. The fluid penetrated only around the borehole, and the penetration area was less than 5% of the total cross-sectional area. The mixture was also injected into control sample B at a pressure of 50 kPa for 10 min, after which the sample was cut vertically to observe the penetration range of the fluid. In sample B, unlike sample A, no upper leakage of the mixture was observed, and a penetration range of ~10% of the total cross-sectional area was confirmed (Fig. 6b).

6.2.2. Fluid penetration by plasma blasting

The laboratory-scale plasma blasting test was conducted in two stages by varying the capacitor capacitance with charging voltages of 10, 20, and 30 kV. In the first step, the capacitance was set to 20 μF, and single plasma blast (SPB) tests and five plasma blasts tests (5PB) were performed on sample A. For sample B, only 5PB tests with capacitance set to 20 and 60 μF were carried out. When the capacitance was 20 μF, the discharge energies were 1, 4, and 9 kJ at discharge voltages of 10, 20, and 30 kV, respectively, and when the capacitance was 60 μF, the discharge energies were 3, 12, and 27 kJ, respectively.

In the SPB test, the mixture was injected for 10 min after one plasma blast. In the 5PB test, plasma blasting was performed five times at 2-min intervals while injecting the mixture for 10 min. After each test, the center of the sample was cut vertically and the area where the mixture had penetrated was measured. The ratio of the fluid penetration area to the total cross-sectional area of the sample was calculated. This value was used as an index for examining the effect of fluid penetration by plasma blasting.

In the SPB test of sample A with the capacity set to 20 μF, the mixture penetrated only a limited area around the borehole (Fig. 7a). The penetration area ratio of the mixture was approximately 16% when the discharge energy was 1 kJ, ~21% when the discharge energy was 4 kJ, and about 25% when the discharge energy was 9 kJ, i.e., as the discharge energy increased, the penetration area ratio also increased. During the SPB test with a discharge energy of 1 kJ, the mixture exhibited only limited penetration around the borehole. With a discharge energy of 4 kJ, the fluid was biased to one side and partially penetrated around the borehole. This result indicates that the physical properties of the sample are not completely homogeneous, despite the consistent compaction process. With a discharge energy of 9 kJ, the borehole collapsed because of the high impact energy, forming a local cavity and a radial small-scale crack.

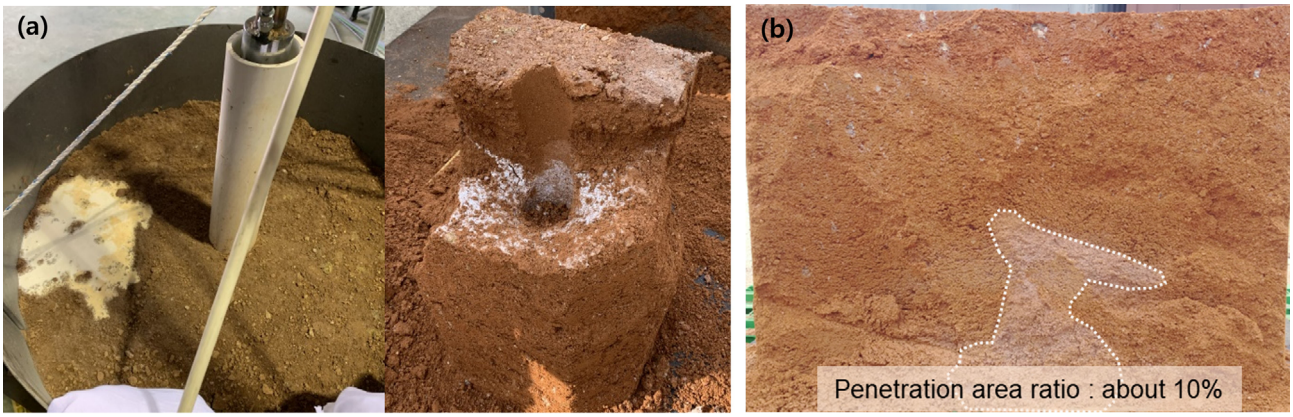

Fig. 6. Fluid penetration without plasma blasting, showing (a) leakage of water mixed with white paint on top of the soil column and formation of a horizontal planar water channel in sample A, and (b) a cross-section of sample B.

https://doi.org/10.1007/s12303-022-0020-3

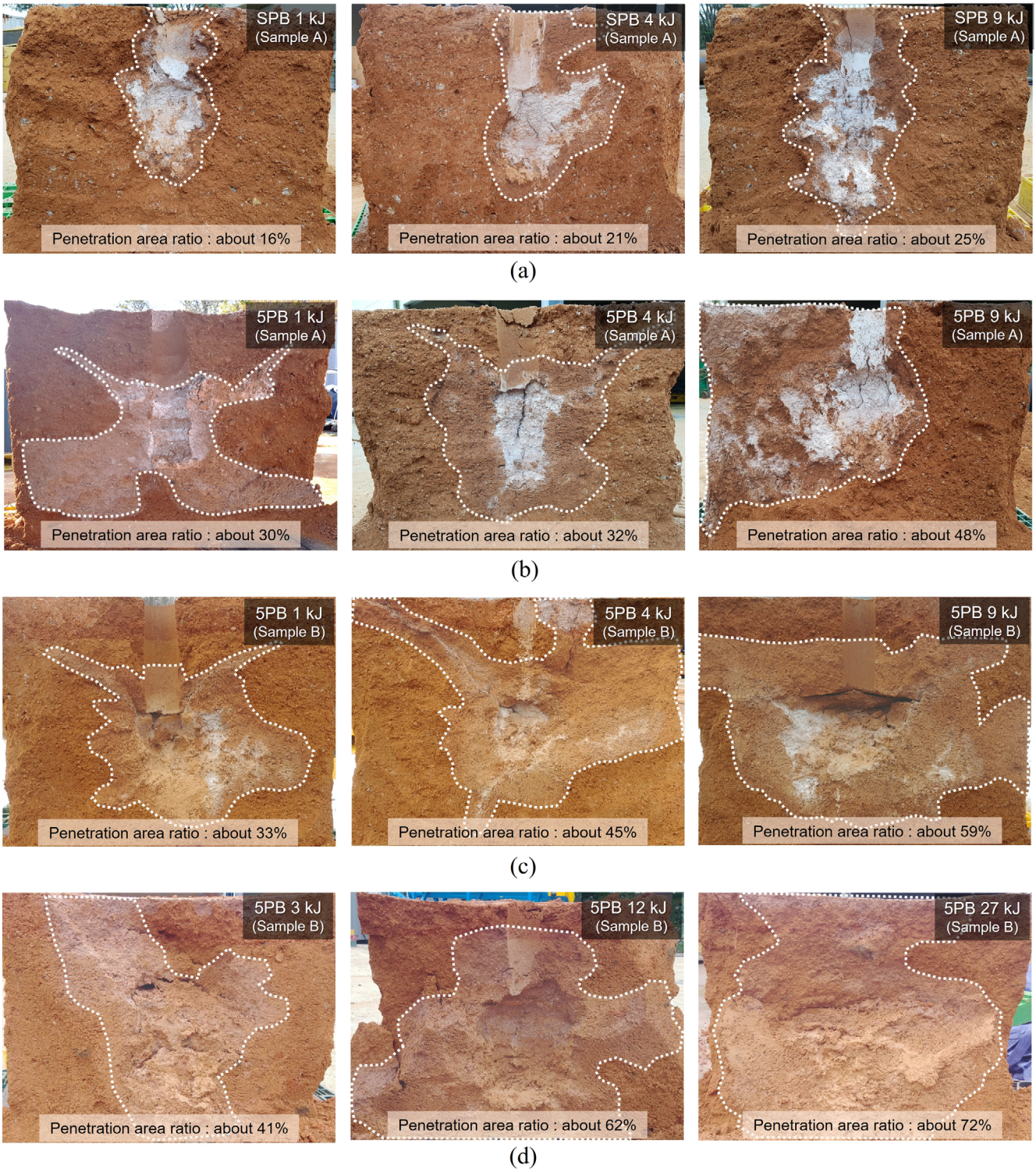

Fig. 7. Fluid penetration area ratios after plasma blasting at the center of the soil column for (a) SPB test on sample A, (b) 5PB test on sample A, (c) 20-μF 5PB test on sample B, and (b) 60-μF 5PB test on sample B.

Overall, the fluid penetration area of sample A for a single plasma blast with a discharge energy of 1 to 9 kJ was approximately 3.2 to 5 times wider than that of the control sample tested only with water pressure.

In the 5PB tests on sample A, no channel was formed and a wide range of mixture penetration was observed (Fig. 7b). The penetration area ratio of the fluid was about 30% at a discharge energy of 1 kJ, ~32% at 4 kJ, and ~48% at 9 kJ, markedly higher

than the values for the SPB test. With a discharge energy of 1 kJ, the fluid penetrated widely into the lower area of the sample and into the upper area in a narrow V-shape. With a discharge energy of 4 kJ, the mixture penetrated in a wide circle centered on the blasting point, and V-shaped penetration occurred at the top of the sample, similar to the 1-kJ 5PB test. With a discharge energy of 9 kJ, the mixture penetrated very widely into the left side of the borehole, and the blasting point notably collapsed because of the very high impact energy (as in the 9-kJ SPB test), forming a wide cavity with a number of cracks around it. Overall, the penetration area of sample A in the 5PB tests with discharge energies of 1–9 kJ was larger by approximately 6–9.6 times relative to injection by only water pressure.

Only 5PB tests with different capacitances were carried out for sample B. The penetration area ratio of the mixture was 33–59% in the 5PB tests with the capacitance set to 20 μF (Fig. 7c). The penetration range increased markedly as the discharge energy increased. In the 1-kJ test, the penetration area of the mixture was almost the same as that of sample A. The penetration pattern in the upper area of the sample was also similar. The penetration area of this sample was approximately 3.3 times wider than that of the control sample tested only with water pressure. In the 4-kJ test, the soil in the blasting area locally collapsed and small irregular cracks were also developed. One side of the sample was penetrated relatively narrowly and irregularly, whereas in the other the fluid penetrated more widely, and some of it flowed out along the cracks. The fluid penetration area of this sample was about 4.5 times wider than that of the control sample. In the 9-kJ test, the fluid penetrated more widely into the sample than in the other tests. As the soil in the blasting point became sludgy as a result of the high discharge energy, large cavities were formed and many cracks occurred. The penetration area was about 5.9 times wider than that of the control sample. Overall, when sample B was subjected to 5PB testing with a discharge energy of 1–9 kJ, the penetration area was approximately 3.3 to 5.9 times larger than that of the control sample (Fig. 7c).

The penetration area ratio of the mixture was approximately 41–72% in the 5PB tests for sample B, in which the capacitor capacitance was increased to 60 μF (Fig. 7d). In the 3-kJ case, after three blasts, the mixture leaked from the upper part of the sample, and the fluid had permeated to the upper part in the vertical section of the sample. In the 12-kJ case, the fluid penetrated most of the middle and lower parts of the sample, and the strong discharge energy made the sample unstable. In the 27-kJ test, which was the highest discharge energy of the plasma blasting tests, the area around the blasting point became widely sludgy, the mixture penetrated into most of the sample cross-section, and the greatest fluid penetration effect was observed. Overall, in the 5PB tests with a discharge energy of 3–27 kJ on sample B, the fluid penetration area in the sample increased by approximately 4.1 to 7.2 times compared with the control sample.

The fluid penetration area ratios of all tests are plotted together in Figure 8. As the discharge energy increases, the penetration area increases. For the same discharge energy, the penetration area increases as the number of blasts increases. The ratio of sample B, which had higher permeability than sample A, is higher than that of sample A. The relationship between the discharge energy and the fluid penetration area ratio of sample B is shown in Figure 9. The ratio increases sharply up as the discharge energy rises up to 9 kJ; however, the rate of increase gradually falls at discharge energies above 9 kJ.

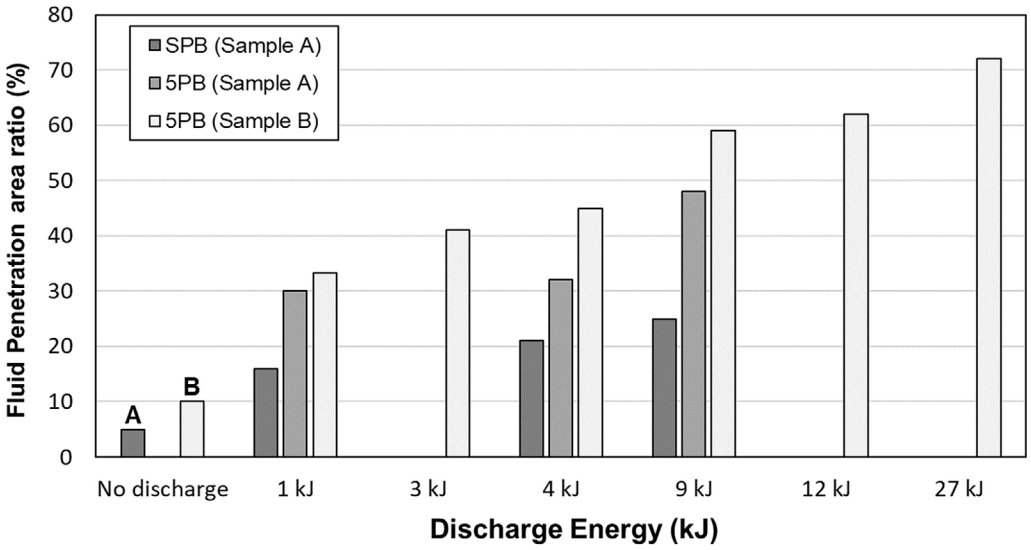

Fig. 8. Fluid penetration area ratios for different numbers of plasma blasts and discharge energies.

https://doi.org/10.1007/s12303-022-0020-3

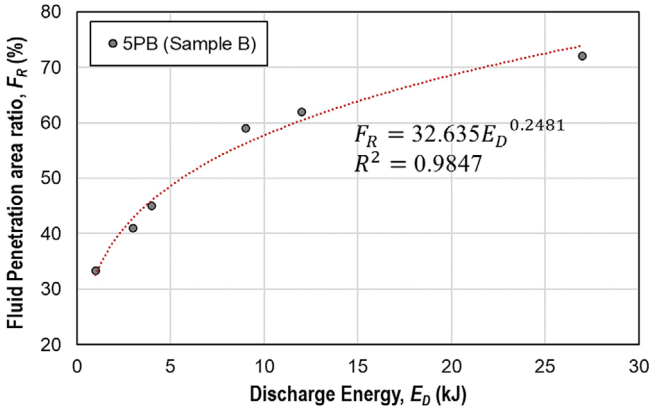

Fig. 9. Relationship between fluid permeation area ratio (F_R) and discharge energy (E_D) for 5PB tests on sample B.

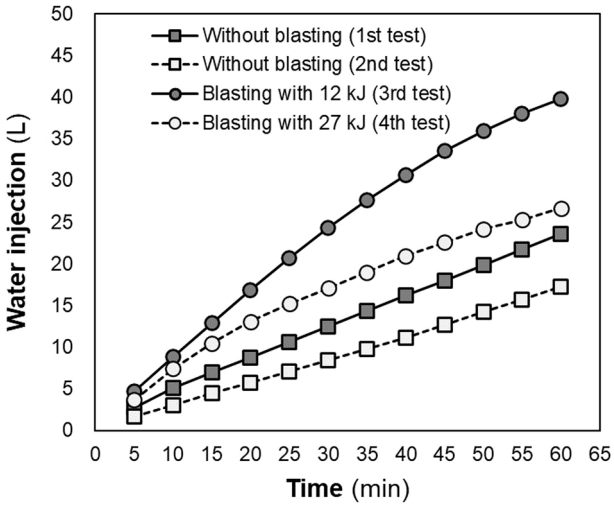

Fig. 10. Cumulative amount of water injected for the single-hole test.

All these results demonstrate that the fluid will penetrate effectively into soil if plasma blasting is conducted. A higher discharge energy and a greater number of plasma blasts will increase fluid penetration; however, too high a discharge energy may cause the soil to become sludgy and produce a cavity in the borehole.

6.2.3. Effect of discharge energy on the penetration radius of fluid

The penetration radius of the fluid was calculated assuming that fluid penetrates in the form of a sphere. The fluid penetration radius (R_p) was calculated from the penetration cross-sectional area (A_p) measured in the laboratory-scale plasma blasting tests (Fig. 7) and is given in Equation (2).

$$R_p = \sqrt{\frac{A_p}{\pi}}. \quad (2)$$

The data for penetration radius according to discharge energy are provided in Table 2. The penetration radius of fluid injected by plasma blasting was greater than that of the fluid injected only by hydraulic pressure. For example, the penetration radius of sample A was 9 cm when injected using only water pressure, whereas the penetration radius of the 1-kJ SPB test of sample A was 15.5 cm, a rise of approximately 72%. For the 5PB tests with the same energy, the penetration radius increased to 21.4 cm, indicating that the penetration radius increases with a greater number of blasts. In both the SPB and 5MPB tests, the higher the discharge energy, the larger the penetration radius. Under the same test conditions, the penetration radius of sample B was approximately 5–18% larger than that of sample A, which had lower permeability than sample B, indicating that the fluid penetration radius is high in the sample with high permeability.

7. FIELD-SCALE PLASMA BLASTING TEST

7.1. Fluid Injection Testing in a Single Borehole

A water injection test was conducted on borehole BH-1 with and without plasma blasting of two different discharge energies. This test was conducted in four steps to examine the effect of plasma blasting and soil moisture content. In the first step, water was injected into the borehole without plasma blasting. Then, water was injected again into the same borehole, in which the soil was wetter than before. In the third test, water was injected

Table 2. Fluid penetration radius caused by plasma blasting

Blasting energy	Fluid penetration radius, R_P (cm)				
	SPB for sample A	5PB for sample A	5PB for sample B	Sample A without plasma blasting	Sample B without plasma blasting
				9.0	12.4
1 kJ	15.5	21.4	22.5		
3 kJ			25.0		
4 kJ	18.1	22.1	26.2		
9 kJ	19.6	27.0	30.0		
12 kJ			30.8		
27 kJ			33.2		

with plasma blasting of 12-kJ discharge energy. Finally, water was injected into the borehole with plasma blasting of 27-kJ discharge energy. In all tests, water was injected for 1 hour with a hydraulic head of 3.3 m, and the interval between tests was 1 hour. Plasma blasting was performed 12 times at 5-min intervals for 1 hour.

The cumulative amount of water injected in each test is shown in Figure 10. The amount of water injected was measured from a water tank with calibration scale of 1 liter. In the first test, a total of 23.6 L was injected and the cumulative amount injected increased linearly with time. In the second test, 17.8 L was injected, a lower amount than that of the first test. The cumulative amount of water injected exhibited a linear increase with time. In the third test, a total of 39.9 L was injected, and the injection rate gradually decreased through time. Finally, 26.7 L was injected with plasma blasting of 27 kJ. The injection rates gradually decreased over time, as in the third test.

The cumulative amount of water injected in the second test was less than that in the first test. The moisture content in the soil before the test might have been low because the experiment was conducted during the dry season and the groundwater level was lower than the test depth. However, the moisture content increased because of water injection during the first test and the soil around the borehole must have become saturated. This result indicates that the amount of water injected into the soil during the first test was abnormally high because of water absorption by the soil. The cumulative amount of water injected in the third test was almost twice as large as that in the first test, although the soil conditions were the same during the third and second tests. This result indicates that plasma blasting improves the efficiency of water injection in soil. The fourth test indicates that too many blasts or blasting with too high a discharge energy may reduce the efficiency of water injection in soil, because disturbance from the plasma blasting causes very fine particles to block pores in the soil, thus decreasing the soil permeability. In the third and fourth tests, the injection rates decreased as the number of blasts increased. This result also proves that too many blasts may reduce the efficiency of water injection in soil.

7.2 Fluid Injection Testing in Different Boreholes

Two different boreholes, BH-2 and BH-3, were selected and water injection tests with and without plasma blasting were conducted to compare the efficiency of fluid injection by plasma blasting. Brine consisting of ~2.5 kg of salt dissolved per 100 L water was injected in BH-2 with a hydraulic head of 3.3 m and plasma blasting, and in BH-3 with only a hydraulic head of 3.3 m. Tests consisting of three steps were conducted in BH-2. One cycle consisted of five blasts within 10 minutes and a 50-minutes break; six cycles were repeated over a 6-hour period. The test was stopped for 12 hours because of safety problems during the night; subsequently, another six cycles were carried out over a 6-hour period. Water was injected for 24 hours continuously. The discharge energy was selected as 12 kJ because too high a discharge energy will reduce the soil permeability (see section 7.1).

7.2.1. Effect of plasma blasting on fluid injection

The cumulative amounts of water injected over 24 hours were measured and the injection rates per hour in boreholes BH-2 and BH-3 were calculated (Fig. 11). The cumulative amount of water injected during the first 6 hours was 122.1 L in BH-2 and 36.8 L in BH-3. The cumulative amount of water injected in BH-2 was 3.4 times more than that in BH-3, indicating that plasma blasting improved fluid injection in soil. During the 12-

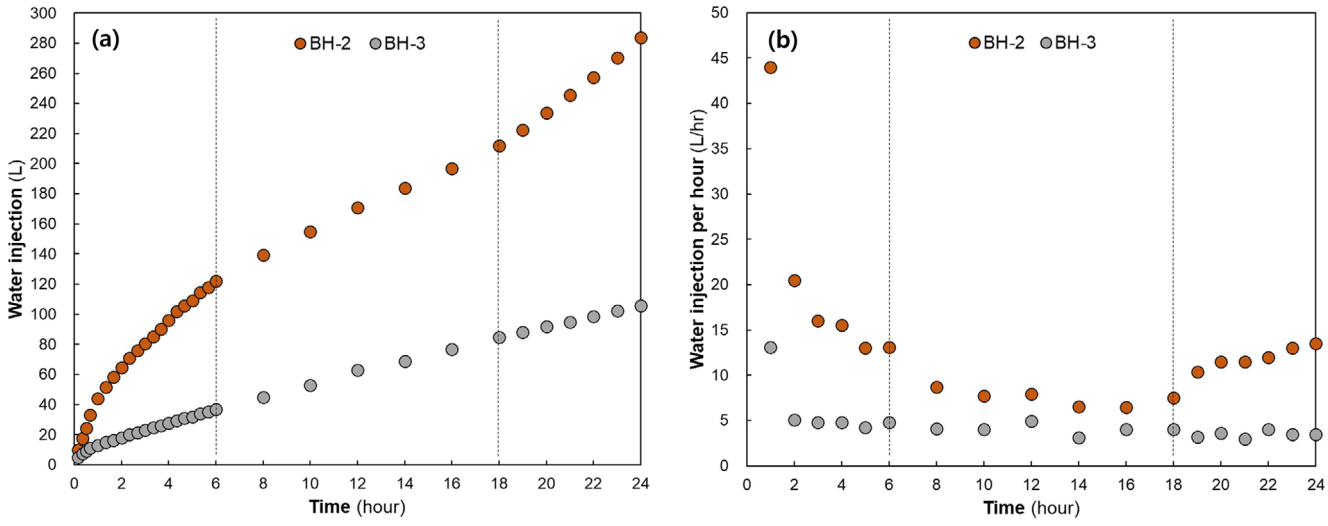

Fig. 11. (a) Cumulative amount of water injected and (b) injection rate per hour.

https://doi.org/10.1007/s12303-022-0020-3

hour break, 89.9 L was injected in BH-2 but 48.2 L in BH-3, indicating that more water will be injected in soil that had previously experienced plasma blasting. However, the amount of water injected in BH-2 was 1.9 times more than that in BH-3, indicating that the ratio will decrease without plasma blasting during injection. During the last 6 hours, 71.9 L was injected in BH-2 (with plasma blasting) and 20.8 L in BH-3 (without plasma blasting). The cumulative amounts decreased in both boreholes but the ratio between the two boreholes was almost the same as that during the first step (Fig. 11a).

Injection rates in BH-3 were almost constant except at the very beginning (Fig. 11b). The very high rates in both BH-2 and BH-3 during the first hour were caused by the original moisture content in the soil being low, so the soil absorbed quite a large amount of water. The almost constant rates after the second hour in BH-3 indicate that no more absorption had occurred along the flow path; thus, the injection rate may be the flow characteristics of soil under the hydraulic head of 3.3 m. The injection rates in BH-2 were higher than those in BH-3 and decreased through time until the fifth hour. From the fifth hour, injection rates seemed to be constant. Higher injection rates in BH-2 than in BH-3 represented expansion of the injection range and/or improvement of soil flow characteristics by plasma blasting. During the 12-hour break, the injection rates in BH-2 were almost constant but higher than those in BH-3, indicating that the flow characteristics of soil were improved by plasma blasting. After the 12-hour break, plasma blasting was performed again in BH-2 and the injection rates increased. However, the injection rate during the 24 hours was almost the same as those during the fifth and sixth hours, indicating that this rate reflected the change in the flow characteristics of soil as a result of plasma blasting.

7.2.2. Analysis of ground vibration

Plasma blasting generates vibrations in the ground, albeit for a short period of time. In some cases, these vibrations have the potential to cause damage to adjacent structures. We evaluated the stability of plasma blasting by measuring the vibrations generated during blasting. NeoBlast's HB-1, which can measure vibration velocities of up to 25.4 cm/s, was used as a vibration measuring device. The vibration caused by plasma blasting was measured four times at a distance of 0.5 m from BH-2. The vibration velocities measured during plasma blasting are listed in Table 3. The vibration velocity measurements and expected damage for different types of soil and bedrock according to Langefors (1978) are provided in Table 4. The vibration velocity during plasma blasting measured in BH-2 is in the range 0.044–0.186 cm/s, a level that does not damage even a very soft soil. Therefore, we conclude that plasma blasting will not cause disturbance or collapse, and that plasma blasting can be applied as an in situ remediation method without damage to adjacent structures even in downtown areas.

7.2.3. Verification of fluid penetration using electrical resistivity

The electrical resistivity distributions around the boreholes before water injection (Phase 1), after 6 hours of water injection (Phase 2), and after 24 hours of water injection (Phase 3) were measured to determine the extent of fluid injection in soil. Because brine was used as the fluid (see section 7.2), the electrical resistivity in the area of fluid penetration should be lower than that before injection. A Syscal Pro (IRIS Instruments) was used for the electrical resistivity survey. Both a dipole-dipole array that had a high horizontal resolution and a modified pole-pole array that showed a strong resistance to induced noise were used (Loke, 1999; Milsom, 2003; Dahlin and Zhou, 2004). The

Table 3. Vibration measured during plasma blasting near BH-2

Number of Plasma blasts	Distance (m)	Vibration velocity (cm/sec)		Vibration range (cm/sec)
		min	max	
1st	0.5	0.077	0.145	0.044–0.186
2nd	0.5	0.044	0.170	
3rd	0.5	0.055	0.186	
4th	0.5	0.102	0.127	

Table 4. Vibration velocity and expected damage level for different types of soil and rock (Langfore, 1978)

	Clay, sand and gravel	Slate and soft limestone	Strong limestone, quartz sandstone, gneiss, granite and basalt	Damage level
Vibration velocity by blasting (cm/s)	0.4–1.8	≤ 3.5	≤ 7.0	No damage
	0.6–3.0	5.5	11.0	Negligible damage
	0.8–4.0	8.8	16.0	Crack generation
	1.2–6.0	≥ 11.5	≥ 23.0	Significant damage

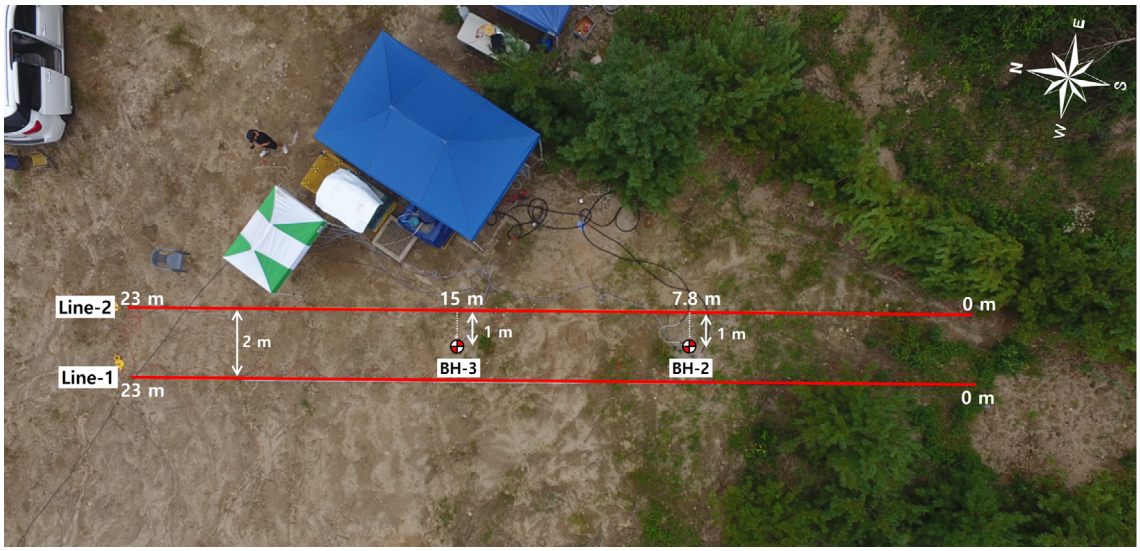

Fig. 12. Layout of boreholes BH-2 and BH-3 and the electrical resistivity survey line.

measurements of apparent resistivity were processed with DIPRO software (Hsgeo, Rep. Korea) using the least square inversion. Two parallel lines (Line 1 and Line 2) located 1 m from both BH-2 and BH-3 and 23 m long were installed (Fig. 12). The distance between the electrodes was 1 m; this arrangement can detect resistivity down to 5 m below the surface. Because the resistivity distribution measured by a modified pole-pole array is quite similar to that measured by a dipole-dipole array, the resistivity distribution measured by a dipole-dipole array is presented here.

A two-dimensional resistivity distribution measured from the dipole-dipole array before water injection (Phase 1) is provided in Figure 13a. The bedrock of the study area is granite and, according to Lee et al. (2012), soil with resistivity less than 200 ohm-m may be classified as an alluvial soil and one with resistivity of 200–500 ohm-m may be completely weathered soil

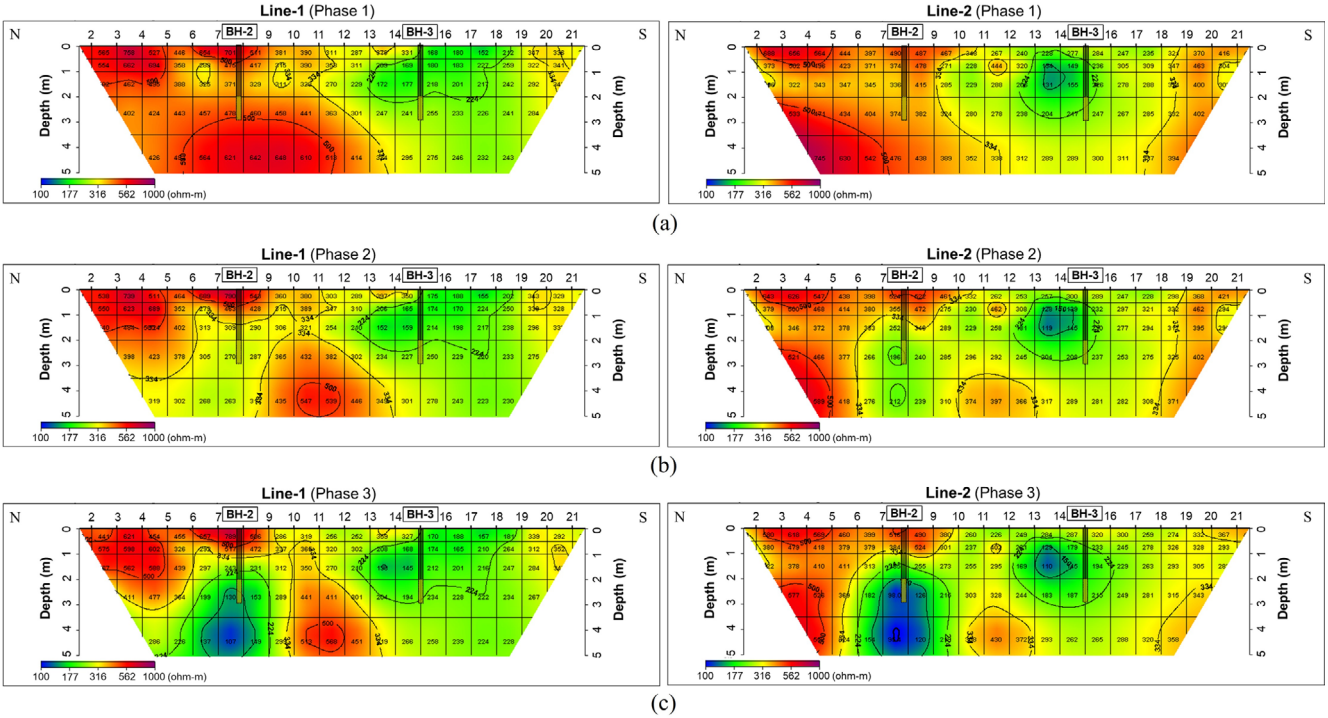

Fig. 13. Two-dimensional resistivity distribution of Line 1 and Line 2 (a) before water injection (Phase 1), (b) after 6 hours of water injection (Phase 2), and (c) after 24 hours of water injection (Phase 3).

https://doi.org/10.1007/s12303-022-0020-3

to highly weathered rock. Resistivity values greater than 500 ohm-m may be classified as highly weathered rock to moderately weathered rock. The resistivity distribution in BH-2 indicates that completely weathered soil to highly weathered rock occurs down to 3 m below the surface, and that highly weathered rock to moderately weathered rock is located below 3 m depth. Very high resistivity at the surface may be caused by local unhomogeneity or a low soil moisture content. Unlike BH-2, the resistivity in BH-3 is lower than 300 ohm-m. The layer above 2 m below the surface may be alluvium, and completely weathered soil lies under the alluvium. The resistivity below line 2 is similar to that below line 1, because lines 1 and 2 are parallel to and close to each other. The resistivity distribution clearly shows a geological boundary at 9–12 m along the line. High resistivity in the left part of Figure 13 represents weathered soil or granite rock, while the low resistivity on the right part of figure represents alluvium, indicating that the right part may represent a valley before deposition of alluvium. BH-2 was selected for the plasma blasting test because the permeability of completely weathered soil is commonly lower than that of alluvium.

The resistivity distributions after 6 hours of water injection (Phase 2) are shown in Figure 13b. Although the resistivity around both BH-2 and BH-3 decreased, the resistivity around BH-2, in which water was injected with plasma blasting, decreased more and to a wider extent than that around BH-3, in which water was injected without plasma blasting, indicating that plasma blasting improved water injection into soil. Although water was injected at 2.0–3.0 m depth below the surface in both BH-2 and BH-3, the resistivity around BH-3 decreased in a small area at 0.5–2.0 m depth. This decrease was caused by local inhomogeneity of the alluvium. The resistivity around BH-2 decreased in a wider and deeper area, from 1.5 to 5.0 m depth and over a radius of more than 2.0 m horizontally. The resistivity decreased more widely in the left area of BH-2 than in the right area; this difference may also have been caused by local inhomogeneity of the soil. The resistivity distributions after 24 hours of water injection (Phase 3) are very similar to those in Phase 2, except that the resistivity had decreased more and to a wider extent (Fig. 13c).

The ratios of the resistivity between after 24 hours of and before water injection clearly show the fluid penetration areas (Fig. 14). A ratio below 1.0 represents a resistivity decrease, indicating brine penetration. The ratios around BH-3 were 0.8–

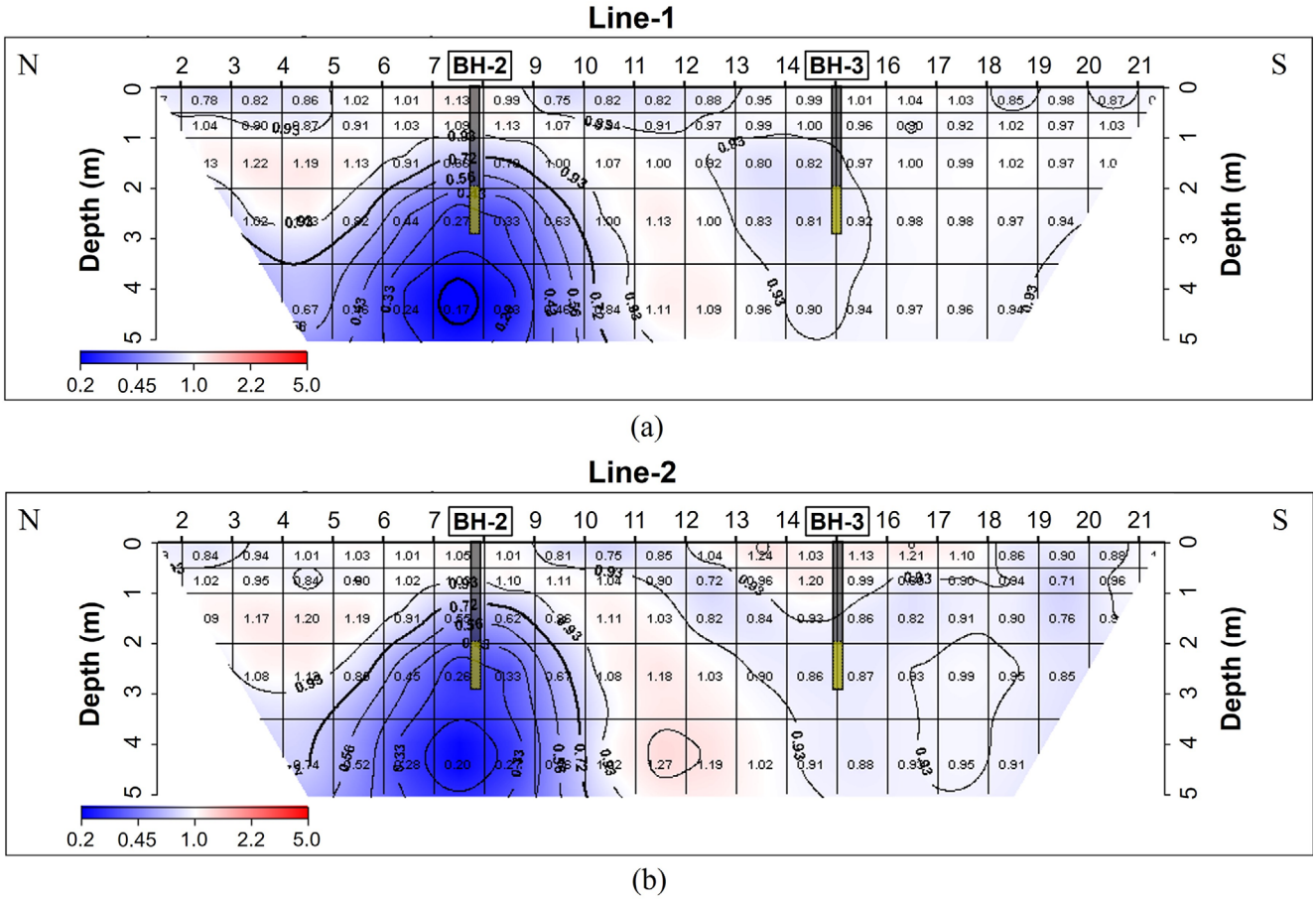

Fig. 14. Contour diagram of the resistivity change ratio between phases 1 and 3 of (a) Line 1 and (b) Line 2.

0.9, suggesting that the amount of fluid penetration was small, so the fluid penetration did not affect the soil resistivity much; however, the range of penetration was quite large, more than 5 m. The ratios around BH-2 decreased markedly, but the range of fluid penetration was smaller than that around BH-3. Low ratios occurred mostly below the plasma blasting depth. This result suggests that fluid penetrated in a limited range and that the fluid flowed downward, rather than horizontally, in the soil, because the fluid injected by plasma blasting caused soil to become saturated in a limited range, and thus the excess fluid flowed downward because of gravity. The injection range resulting from plasma blasting with a discharge energy of 12 kJ might be 2 to 3 m in radius. If the discharge energy changes, the injection range will also change. All these results indicate that plasma blasting improves fluid injection into soil.

8. SUMMARY AND CONCLUSION

To determine the applicability of plasma blasting for in situ remediation of contaminated soil, a plasma blasting device was manufactured and laboratory and field tests were conducted. In the plasma blasting equipment, the voltage charged in the capacitor and the discharge voltage at the tip of the discharge probe were almost the same as each other, and the current increased linearly up to a maximum of ~60 kA as the discharge voltage increased. This result shows that the discharge energy at the time of plasma blasting can be predicted from only the charging voltage of the plasma blasting device. In a laboratory test using a columnar soil sample, the fluid penetration area ratio was less than 5% when the fluid was injected with only ~50 kPa of water pressure without plasma blasting into sample A. The penetration area ratio of sample B, which had relatively higher permeability than sample A, was approximately 10%. This finding demonstrates that restoring low-permeability soil by in situ soil cleaning using only water pressure is very difficult. In contrast, in the plasma blasting test for sample A, the penetration area ratio of the fluid was 16–25% after a single blast and 30–48% after five consecutive blasts. These results mean that, for sample A, plasma blasting increases the penetration area by 3.2 to 9.6 times relative to that of fluid injection by only hydraulic pressure. The higher the discharge energy during plasma blasting, the higher the penetration area ratio: for five blasts, the penetration area ratio was 1.5 to 1.9 times larger than that for a single blast. For sample B, which had relatively higher permeability, the penetration area ratio of the fluid was 33–72%, and the penetration area was expanded by 3.3 to 7.2 times relative to fluid injection by water pressure only. These test results show that plasma blasting increases the fluid penetration, and the penetration area of the fluid increases as the discharge energy and number of blasts increases. The calculated penetration radius (Rp), assuming spherical fluid penetration, was 9 to 12.4 cm in a sample injected with only water pressure, and increased to 27.0 to 33.2 cm with plasma blasting, i.e., the penetration effect of the fluid was improved by 168–200%. The penetration radius resulting from plasma blasting was calculated to be larger for sample B, which had higher permeability, but the improvement in penetration radius was larger for the lower-permeability sample A. This result means that the improvement in fluid penetration by plasma blasting is greater in samples with low permeability. In the field test conducted in borehole BH-1, 17.8–23.6 L of water was injected during a 1-hour period when only hydraulic pressure was applied. The amount injected was less when the borehole was in a wet state than when it was dry. When plasma blasting was performed with discharge energies of 12 kJ and 27 kJ, 39.9 L and 26.7 L of water were injected over a 1-hour period, respectively, and the water injection effect was improved by 55–131% compared with the case in which only hydraulic pressure was used. The test results for BH-1 showed that the fluid penetration effect can be reduced when the discharge energy is too high in field tests, unlike in the laboratory tests, in which greater discharge energy was associated with greater fluid penetration. The amount of water injected during a 24 hour period was compared for borehole BH-2, to which plasma blasting was applied, and borehole BH-3, in which fluid was injected only by hydraulic pressure. The range of water diffusion was identified by conducting an electrical resistivity survey. Over a 24-hour period, 283.9 L of water was injected into BH-2 and 105.8 L of water was injected into BH-3; thus, plasma blasting improved the water injection efficiency by approximately 170%. In the electrical resistivity survey, there was no marked change in the resistivity of the ground around BH-3 after 24 hours of water injection; however, in the ground around BH-2 (to which plasma blasting was applied), the specific resistance decreased below 1 m depth and decreased by more than 80% below 3 m depth, confirming that water had diffused from the borehole to a distance of at least 2 m.

In conclusion, we confirmed that plasma blasting increases the fluid penetration rate in both small-scale soil samples and in the actual ground, which is a semi-infinite medium under in situ stress. Therefore, we conclude that the plasma blasting method has sufficient utility value as an in situ remediation method for contaminated sites.

ACKNOWLEDGMENTS

This study was supported by Korea Environment Industry & Technology Institute (KEITI) through the Sub-Surface Environmental Management (SEM) Project, funded by the Korea Ministry of Environment (MOE) (Grant 2020002480010).

https://doi.org/10.1007/s12303-022-0020-3

REFERENCES

Aggelopoulos, C.A., Hatzisymeon, M., Tataraki, D., and Rassias, G., 2020, Remediation of ciprofloxacin-contaminated soil by nanosecond pulsed dielectrical barrier discharge plasma: influencing factors and degradation mechanisms. Chemical Engineering Journal, 393, 124768. https://doi.org/10.1016/j.cej.2020.124768

Baltazar-Lopez, M., Brandhorst, H., Burell, Z., and Heffernan, M., 2009, Analysis and simulations of low power plasma blasting for processing lunar materials. 7th International Energy Conversion Engineering Conference, Denver, Aug. 2–5, AIAA 2009-4550. https://doi.org/10.2514/6.2009-4550

Best, S., Baltazar-Lopez, M.E., Burell, Z.M., Brandhorst, H.W., Heffernan, M.E., and Rose, M.F., 2008, A low power approach for processing lunar materials. Proceedings of the 6th International Energy Conversion Engineering Conference (IECEC), Cleveland, Jul. 28–30, AIAA 2008-5710. https://doi.org/10.2514/6.2008-5710

Chen, W., Maurel, O., Reess, T., Ferron, A., La Borderie, C., Pijaudier-Cabot, G., and Rey-Bethbeder, F., 2012, Experimental study on an alternative oil stimulation technique for tight gas reservoirs based on dynamic shock waves generated by pulsed arc electrohydraulic discharges. Journal of Petroleum Science and Engineering, 88, 67–74.

Christiansen, C. and Wood, J.S.A., 2006, Environmental fracturing in clay till deposits. Master Thesis, Institute of Environment & Resources, Technical University of Denmark, Kongens Lyngby, 253 p.

Dahlin, T. and Zhou, B., 2004, A numerical comparison of 2D resistivity imaging with 10 electrode arrays. Geophysical Prospecting, 52, 379–398.

EPA, 1995, In situ remediation technology status report: hydraulic and pneumatic fracturing. EPA Report, EPA542-K-94-005, United States Environmental Protection Agency, Washington DC, 16 p.

EPA, 2004, Cleaning up the nation's waste sites: markets and technology trends (2004 edition). EPA Report, EPA-542-R-04-015, United States Environmental Protection Agency, Washington DC, 338 p.

EPA, 2007, Treatment technologies for site cleanup: annual status report (12th edition). EPA Report, EPA-542-R-07-012, United States Environmental Protection Agency, Washington DC, 290 p.

Fawzy, E.M., 2008, Soil remediation using in situ immobilisation techniques. Chemistry and Ecology, 24, 147–156.

Ferrucci, A., Vocciante, M., Bagatin, R., and Ferro, S., 2017, Electrokinetic remediation of soils contaminated by potentially toxic metals: dedicated analytical tools for assessing the contamination baseline in a complex scenario. Journal of Environmental Management, 203, 1163–1168.

Frank, U. and Barkley, N., 1995, Remediation of low permeability subsurface formations by fracturing enhancement of soil vapor extraction. Journal of Hazardous Materials, 40, 191–201.

Hammon, J., Hopwood, D., Klatt, M., and Tatman, T., 2001, Electrical pulse rock sample disaggregator. 28th IEEE International Conference on Plasma Science and 13th IEEE International Pulsed Power Plasma Science, Las Vegas, Jun. 17–22, p. 1142–1145. https://doi.org/10.1109/PPPS.2001.1001747

Huguenot, D., Moisset, E., van Hullebusch, E.D., and Oturan, M.A., 2015, Combination of surfactant enhanced soil washing and electro-Fenton process for the treatment of soils contaminated by petroleum hydrocarbons. Journal of Environmental Management, 153, 40–47.

Ikkurthi, V.R., Tahiliani, K., and Chaturvedi, S., 2002, Simulation of crack propagation in rock in plasma blasting technology. Shock Waves, 12, 145–152.

Jang, H.S., Kim, K.J., Song, J.Y., An, S.G., and Jang, B.A., 2020, An experimental study to improve permeability and cleaning efficiency of oil contaminated soil by plasma blasting. The Journal of Engineering Geology, 30, 557–575. (in Korean with English abstract)

Kang, H.C., Han, B.G., Kim, J.D., Seo, S.W., Shin, C.H., and Park, J.S., 2017, Evaluation of soil flushing column test for oil-contaminated soil treatment. Clean Technology, 23, 302–307. (in Korean with English abstract)

Langefors, U. and Kihlström, B., 1978, The Modern Technique of Rock Blasting (3rd edition). Wiley, New York, 438 p.

Lee, K.H., Seo, H.J., Park, J.H., Ahn, H.Y., Kim, K.S., and Lee, I.M., 2012, A study on correlation between electrical resistivity obtained from electrical resistivity logging and rock mass rating in-situ tunnelling site. Journal of Korean Tunnelling and Underground Space Association, 14, 503–516. (in Korean with English abstract)

Lhotský, O., Kukačka, J., Slunský, J., Marková, K., Nemecek, J., Knytl, V., and Cajthaml, T., 2021, The effects of hydraulic/pneumatic fracturing-enhanced remediation (FRAC-IN) at a site contaminated by chlorinated ethenes: a case study. Journal of Hazardous Materials, 417, 125883. https://doi.org/10.1016/j.jhazmat.2021.125883

Li, O.L.H., Chang, J.S., and Guo, Y., 2011, Pulsed arc electrohydraulic discharge characteristics, plasma parameters, and optical emission during contaminated pond water treatments. IEEE Electrical Insulation Magazine, 27, 8–17.

Li, Z., Yu, J.W., and Nerentnieks, I., 1996, A new approach to electrokinetic remediation of soils polluted by heavy metals. Journal of Contaminant Hydrology, 22, 241–253.

Liu, J.W., Wei, K.H., Xu, S.W., Cui, J., Ma, J., Xiao, X.L., Xi, B.D., and He, X.S., 2021, Surfactant-enhanced remediation of oil-contaminated soil and groundwater: a review. Science of the Total Environment, 756, 144142.

Loke, M.H., 1999, Electrical Imaging Surveys for Environmental and Engineering Studies: A Practical Guide to 2D and 3D Surveys. Geotomo Software, Gelugor, Malaysia, 70 p.

Maurel, O., Reess, T., Matallah, M., Ferron, A.D., Chen, W., Borderie, C.L., Pijaudier-Cabot, G., Jacques, A., and Rey-Bethbeder, F., 2010, Electrohydraulic shock wave generation as a means to increase intrinsic permeability of mortar. Cement and Concrete Research, 40, 1631–1638.

Milsom, J., 2003, Field Geophysics (3rd edition). Wiley, New York, 244 p.

Park, B.S. and Yeo, S.C., 1971, Explanatory text of the geological map of Moggye sheet (scale 1: 50,000). Korea Institute of Geoscience and Mineral Resources, Daejeon, Republic of Korea, 24 p. (in Korean with English abstract)

Riu, H., Jang, H.S., Lee, B., Wu, C., and Jang, B.A., 2019, Laboratory-scale fracturing of cement and rock specimen by plasma blasting. Episodes, 42, 213–223.

Rosestolato, D., Bagatin, R., and Ferro, S., 2015, Electrokinetic remediation of soils polluted by heavy metals (mercury in particular). Chemical Engineering Journal, 264, 16–23.

Santos, E.V., Souza, F., Saez, C., Cañizares, P., Lanze, M.R.V., Martinez-Huitle, C.A., and Rodrigo, M.A., 2016, Application of electrokinetic soil flushing to four herbicides: a comparison. Chemosphere, 153, 205–211.

Schuring, J.R., Kosson, D.S., Fitzgerald, C.D., and Venkatraman, S., 1996, Pneumatic fracturing and multicomponent injection enhancement of in situ bioremediation. United States Patent, Patent No 5,560,737, Washington DC, 23 p.

Suthersan, S., 1999, Remediation Engineering: Design Concepts. CRC Press, Boca Raton, 237 p.

Touya, G., Reess, T., Pecastaing, L., Gibert, A., and Demens, P., 2006, Development of subsonic electrical discharges in water and measurements of the associated pressure waves. Journal of Physics D: Applied Physics, 39, 5236–5244.

Venkatraman, S.N., Schuring, J.R., Boland, T.M., Bossert, I.D., and Kosson, D.S., 1998, Application of pneumatic fracturing to enhance in-situ bioremediation. Journal of Soil Contamination, 7, 143–162.

Yan, F., Lin, B., Zhu, C., Guo, C., Zhou, Y., Zou, Q., and Liu, T., 2016, Using high-voltage electrical pulses to crush coal in an air environment: an experimental study. Powder Technology, 298, 50–56.

Yang, J.W. and Lee, Y.J., 2007, Status of soil remediation and technology development in Korea. Korean Chemical Engineering Research, 45, 311–318. (in Korean with English abstract)

Zhan, J., Liu, Y., Cheng, W., Zhang A., Li, R., Li, X., Ognier, S., Cai, S., Yang, C., and Liu, J., 2018, Remediation of soil contaminated by fluorene using needle-plate pulsed corona discharge plasma. Chemical Engineering Journal, 334, 2124–2133.

Zhu, L., He, Z.H., Li, P., Xu, T.S., Zhao, H., Zhao, X.F., and Gao, Z.W., 2013, The research on the pulsed arc electrohydraulic discharge and its application in treatment of the ballast water. Journal of Electrostatics, 71, 728–733.

https://doi.org/10.1007/s12303-022-0020-3